Resource Management of Forested Wetlands: Hurricane Impact and Recovery Mapped by Combining Landsat TM and NOAA AVHRR Data

Elijah W. Ramsey III, Dal K. Chappell, Dennis M. Jacobs, Sijan K. Sapkota, and Dan G. Baldwin

Abstract

A temporal suite of NOAA Advanced Very High Resolution Radiometer (AVHRR) images, transformed into a vegetation biomass indicator, was combined with a single-date classification of Landsat Thematic Mapper (TM) to map the association between forest type and hurricane effects. Hurricane effects to the forested wetland included an abrupt decrease and subsequent increase in biomass. The decrease was associated with hurricane impact and the increase with an abnormal bloom in vegetation in the impacted areas. Impact severity was estimated by differencing the biomass maps before and immediately (3 days) after the hurricane. Recovery magnitude was estimated by differencing the biomass maps from immediately (3 days) after and shortly (1.5 months) after the hurricane. Regions of dominantly hardwoods suffering high to moderate impacts and of dominantly cypress-tupelos suffering low impacts identified in this study corroborated findings of earlier studies. Conversely, areas not reported in previous studies as affected were identified, and these areas showed a reverse relationship, i.e., highly impacted cypress-tupelo and low or moderately impacted hardwoods. Additionally, generated proportions of hardwood, cypress-tupelo, and open (mixed) forests per each 1-km pixel (impact and recovery maps) suggest that regions containing higher percentages of cypress-tupelos were more likely to have sustained higher impacts. Visual examination of the impact map revealed a spatial covariation between increased impact magnitudes and river corridors dominated by open forest. This spatial association was corroborated by examining changes in the percentage of open forest per 1-km impact pixel; the percentage of open forest peaked at moderate to high impacts. The distribution of recovery supported the impact spatial distribution; however, the magnitudes of the two indicators of hurricane effects were not always spatially dependent. Converse to univariate statistics describing all forested area within the basin, higher recoveries tended to be related to higher percentages of hardwoods. Lower recoveries, on the other hand, tended to be related to forests with nearly equal percentages of hardwoods and cypress-tupelo.

Introduction

Traditionally, satellite remote sensing studies of natural resources have relied on sensors such as the Landsat Thematic Mapper (TM), Multispectral Scanner (MSS), SPOT XMS, and Advanced Very High Resolution Radiometer (AVHRR). Users requiring relatively high spectral and spatial resolutions primarily have used TM, MSS, or SPOT, while those requiring high temporal resolutions (<16 days) and large regional coverages have used AVHRR (Lulla and Mausel, 1983; Roughgarden *et al.*, 1991; Wickland, 1991; Eastman and Fulk, 1993; Andres *et al.*, 1994; Ripple, 1994; Zhu and Evans, 1994). Special requests can trigger an increased collection frequency of SPOT imagery. When warranted, however, use of AVHRR imagery offers the advantage of collections twice daily over a large region and at a low cost. Finally, while the value of TM, MSS, SPOT, and AVHRR sensors in mapping natural resources is well documented, often resource managers require data that have the combined spatial and spectral resolution of TM, MSS, and SPOT, and the temporal resolution and regional coverage of AVHRR. To achieve this combination of resolutions and coverages, remote sensing research in natural resources has focused on integrating different sources of sensor data.

Various techniques, including visual comparisons, linear regressions, and overlays, have been applied to integrate the spectral and temporal scales of TM, MSS, SPOT, and AVHRR sensors (e.g., Settle and Drake, 1993; Ehrlich *et al.*, 1994; Chavez and MacKinnon, 1994; Moody and Woodcock, 1994). Usually, however, larger scale optical imagery is used to verify AVHRR land-cover and land-use classes. These verifications are valuable to integration, but most users emphasize integration at a single time, neglecting the high temporal resolution advantage of the AVHRR sensor. Yet, this temporal resolution is especially important for monitoring rapid changes and recovery (e.g., from storm impact, herbivory, or fire) in forested areas. In these cases, a dynamic remote sensing tool is required with moderate to high temporal (at least weekly), spatial, and spectral (blue, green, red, near infrared, and short-wave bandwidths) resolutions. Presently, no single sensor offers the necessary combination of resolutions.

Hurricane Andrew, which struck Louisiana on 26 Au-

E.W. Ramsey III and D.K. Chappell are with the U.S. Geological Survey, Biological Resources Division, National Wetlands Research Center, 700 Cajundome Blvd., Lafayette, LA 70506 (elijah_ramsey@usgs.gov).

D.M. Jacobs is with the U.S. Forest Service, Southern Research Station, Forest Inventory and Analysis, Starkville, MS 39760-0928.

S.K. Sapkota is with Johnson Controls World Services Inc., 700 Cajundome Blvd., Lafayette, LA 70506.

D.G. Baldwin is with the Colorado Center for Astrodynamics Research, Box 431, University of Colorado, Boulder, CO 80309.

Photogrammetric Engineering & Remote Sensing, Vol. 64, No. 7, July 1998, pp. 733–738.

0099-1112/98/6407–733$3.00/0

gust 1992, provided a practical application for a combined use of AVHRR and TM data. To map the hurricane impact to a forested wetland, AVHRR images were transformed into a normalized difference vegetation index (NDVI) as an indicator of vegetation changes (Ramsey *et al.*, 1997). Temporal curves of mean NDVIs for three forest sites for the dates before and shortly after the hurricane's passage and aggregate curves of the impacted forest to an undisturbed forest were compared. These comparisons corroborated the atypical phenology of the impacted forested wetland and directly related the cause to the hurricane passage.

Changes in a vegetation index generated from the AVHRR imagery seemed to reflect differences in damage severity and type (Ramsey *et al.*, 1997). This similarity suggested that not only damage extent but also information on damage severity and type may be extracted from the temporal pattern of the vegetation indicator derived from the AVHRR imagery. Further, if forest type could be derived from prehurricane TM imagery, a link could be made between damage severity and type and forest type. Such information could help resource managers monitor and maintain forested wetland habitats and help researchers develop models of storm impact to wetland forests.

The goal of this study was to integrate information gained from a temporal suite of AVHRR images with a prehurricane TM image. The first objective was to generate a classified map of the forest area by using a TM image from before the hurricane; the second was to derive a hurricane impact and recovery map of the forested area from the AVHRR imagery compiled during a previous study (see Ramsey *et al.*, 1997); and the third was to relate information in the AVHRR-produced impact and recovery maps to forest type extracted from the prehurricane TM image.

Methods

National Oceanic and Atmospheric Administration (NOAA 11) AVHRR images were acquired for time periods before and after Hurricane Andrew (Ramsey *et al.*, 1997). Four 1992 AVHRR images, 30 June (composite of 23 June and 6 July images), 29 August (three days after the hurricane passage), and 19 October were used for this study. Persistent cloud cover prevented the use of more AVHRR images covering the Atchafalaya River basin (Ramsey *et al.*, 1997). One image from 16 August 1992, however, was cloud free over the southern third of the basin. Within this area (represented by a southern site [Ramsey et al., 1997]), the decrease in NDVI was about 0.11 between the 30 June and 29 August images and about 0.16 between the 16 August and 29 August images.

AVHRR images were georeferenced to a conic projection at a 1.1-km resolution and converted to reflectance estimates by using software developed at the Colorado Center for Astrodynamics Research at the University of Colorado (Rosborough *et al.*, 1994). Image registration accuracies were estimated at about ± 1 pixel. The reflectance images were converted to NDVI and scaled (Equations 1, 2, and 3) for further analyses (Eidenshink, 1992; Samson, 1993; Ramsey *et al.*, 1997): i.e.,

$$\text{Scaled: NDVI}^* = ((\text{AVHRR}_{\text{NIR}} - \text{AVHRR}_{\text{RED}})/(\text{AVHRR}_{\text{NIR}} + \text{AVHRR}_{\text{RED}}) + 1) \times 127.5 \quad (1)$$

$$\text{Differenced: } \Delta\text{NDVI} = \text{NDVI}_{\text{Jun}} - \text{NDVI}_{\text{Aug}} \quad (2)$$

$$\text{Scaled Differenced: } \Delta\text{NDVI}^* = (\text{NDVI}_{\text{Jun}} - \text{NDVI}_{\text{Aug}}) \times 127.5 \quad (3)$$

In the following discussion, impact and recovery NDVIs refer to the difference between two dates by applying Equation 3.

A progressive clustering technique was used to categorize the georeferenced TM image (Jensen *et al.*, 1987; Ramsey and Laine, 1997). Output categories were water, hardwoods, cypress-tupelo, mixed open canopy, floating vegetation, and other (Plate 1). Following discussions with foresters about advantageous forest classes, separation of willows and other hardwoods was attempted; however, these forest types were not separable. The mixed open canopy class included willow or cypress-tupelo with more open canopies and floating vegetation. A three-by-three majority sieve was used on the final classified map to reduce classification error and noise (Jensen *et al.*, 1994).

A class-stratified random sampling technique using 50 samples per class and near-concurrent 1:24,000-scale color infrared (CIR) photography as reference data were used to generate classification error estimates (Congalton, 1988; Congalton, 1991; Janssen and van der Wel, 1994). Overall, 85.9 percent of the samples were correctly classified and a 0.81 kappa estimate was found. Another comparison to land-cover type at 175 forest inventory and analysis sites within the Atchafalaya Basin found an 82.8 percent classification accuracy and a 0.76 kappa estimate.

Differencing of the NDVI images was used to produce the impact and recovery maps of the Atchafalaya Basin forested area (Figures 1a and 1b). As mentioned, the difference between NDVIs generated from the 16 August image of the lower third of the basin and the 29 August image indicated that the drop in NDVI was more dramatic (by about 6 scaled NDVI units) than that represented by the 30 June and 29 August differences. In addition, however, in 1991 and 1993, NDVI decreases typifying nonimpact years were about 6 for this area. As a compromise, impact magnitudes were estimated to equal the difference of the 30 June and 29 August NDVI values, but, without collateral information, differences lower than about 6 were questionable. This lower limit based on non-impact years was expected to account for any changes in NDVI not related to hurricane wind damage (e.g., leaf wilt, incomplete normalization of atmospheric influences, changing water levels under mostly closed canopies). Recovery magnitudes were estimated as the difference of the 19 October and 29 August NDVI values (only magnitudes above zero were considered).

Presumably, higher impacts could result from either more widespread damage or isolated areas of severe damage within the 1-km pixels. Interpretation of post-hurricane January 1993 1:24,000-scale CIR photography showed evidence for severe damage (i.e., downed to partially uprooted trees) in high impact areas identified in this study. Because of the leaf-off conditions and the lapse of time since the hurricane passage, however, identification of damage in the photography was sometimes difficult. We suggest that high impact pixels are a result of some portion of the forest within the pixel being severely damaged and the surrounding area impacted to some lessor degree, with the lower impact magnitude describing the less occurrence of severe impact within the pixel. Regions of lower impacts, however, probably did not contain areas of severe damage but were mostly areas of defoliation and possible limb loss. Increase in recovery magnitudes were considered in the same way. High recoveries were most likely associated with widespread increase in biomass related to defoliation or limb loss, and possibly some downed or uprooted trees, throughout the 1-km pixel.

For comparison to the TM image, the AVHRR NDVI images were subset to an area coincident with the Atchafalaya River Basin extent and resampled with a nearest-neighbor selection criteria to a 25-m spatial resolution (PCI, 1993). Subsequently, a crosstabulation of the impact and recovery magnitudes was generated for open, cypress-tupelo, and hardwood classes. This crosstabulation allowed the calculation of univariate statistics by forest type generalized for the entire basin. To elucidate the spatial association between impact and recovery with forest type, however, a clearer measure was

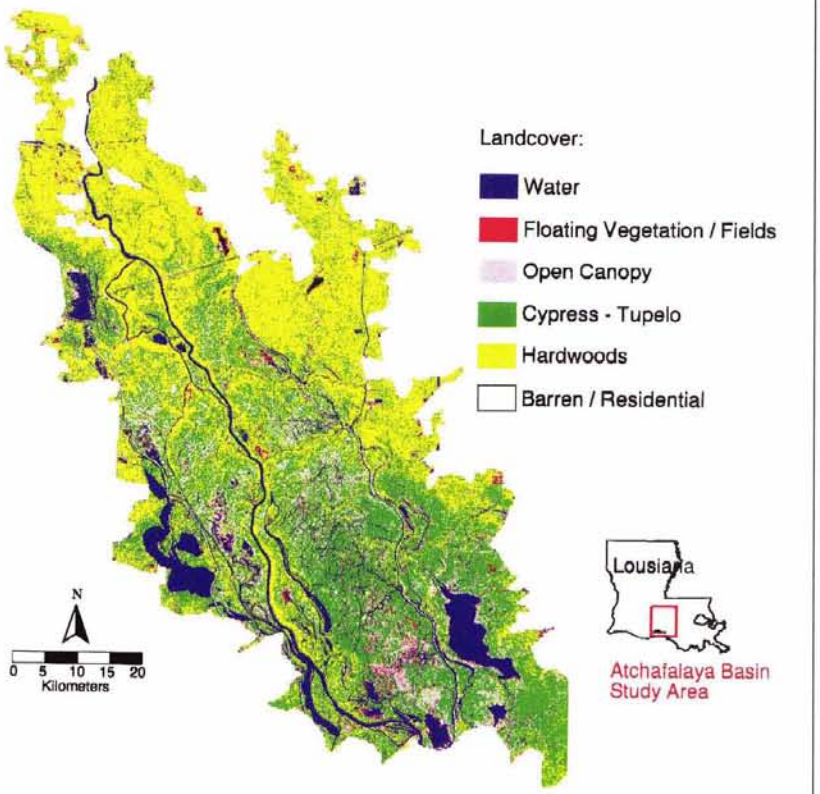

Plate 1. A classified map of the Atchafalaya River basin. The open canopy class depicts areas of more open canopy containing a mix of hardwoods and cypress-tupelos.

needed. Generation of this measure required the use of an overlay procedure.

The overlay method involved first indexing each AVHRR pixel with a particular value before resampling. This index value allowed the spatial linkage between each 1-km impact and recovery pixel and 25-m classified TM pixel to be retained. The number of pixels of each land-cover class within each 1-km pixel was calculated. Percentages of each forest type were then generated by dividing the number of 25-m pixels of each forest type per 1-km pixel by the total number of 25-m forest pixels in the associated 1-km pixel. Univariate statistics were generated from the sets of percentages. Normalized by the total number of 25-m pixels per 1-km pixel, 1-km pixels containing over 15 percent water or floating vegetation and boundary pixels lying less than 75 percent within the basin were excluded from the analysis.

Results

Spatially, the distribution of relatively higher impact magnitudes was fairly concentrated along the southwestern edge of the basin, closely following the mixed hardwoods and cypress-tupelo corridor along the Atchafalaya River (Plate 1 and Figure 1a). Another area of concentrated impact occurred in the southeastern corner of the basin. More widespread lower impact occurred to the north, covering the entire midsection of the basin. Generally, this pattern of impact reflects the initial northward trend and then eastern turn of the hurricane. Less impact was predicted in the northwest area of the basin, which was at or to the left of the hurricane track as it turned eastward. Another area of low impact occurred in the southcentral area of the basin. This area is typified by a nearly uniform coverage of cypress-tupelo with some open canopy areas. Less impact in this area could support the theory that cypress-tupelo forests are more resistant to wind damage than are hardwood forests (Doyle *et al.*, 1995).

The spatial distribution of recoveries generally follows the spatial distribution of impacts; however, magnitudes do not appear to necessarily covary (Figures 1a and 1b). Recovery magnitudes were highest along the Atchafalaya River corridor and the midsection of the basin. River corridors are, in general, lined with willows and other hardwoods, while the midsection of the basin is cypress-tupelo dominated but still contains a substantial mixture of hardwoods. As in the impact distribution, an isolated area of higher recovery magnitudes was located in the southeast corner of the basin.

Generalized for the entire basin and including all pixels (impact and nonimpact), the means and standard deviations of impact and recovery magnitudes were 10.6 and 8.8, and 5.0 and 10.6, respectively. These univariate statistics suggest a higher change in mean NDVI between June and August than between August and October. Impact magnitudes crosstabulated to each forest type resulted in overall basin means and standard deviations of 9.8 and 7.2 for hardwoods, 10.9 and 8.1 for cypress-tupelo, and 10.2 and 8.6 for open. Recovery means and standard deviations were 3.2 and 9.9 for hardwoods, 6.6 and 9.8 for cypress-tupelo, and 6.7 and 9.4 for open. These basin-wide statistical measures seem to imply a nearly equal average impact to all three forest classes, while recovery distribution measures imply higher recovery among the cypress-tupelo and open classes and lower recovery in the hardwood class.

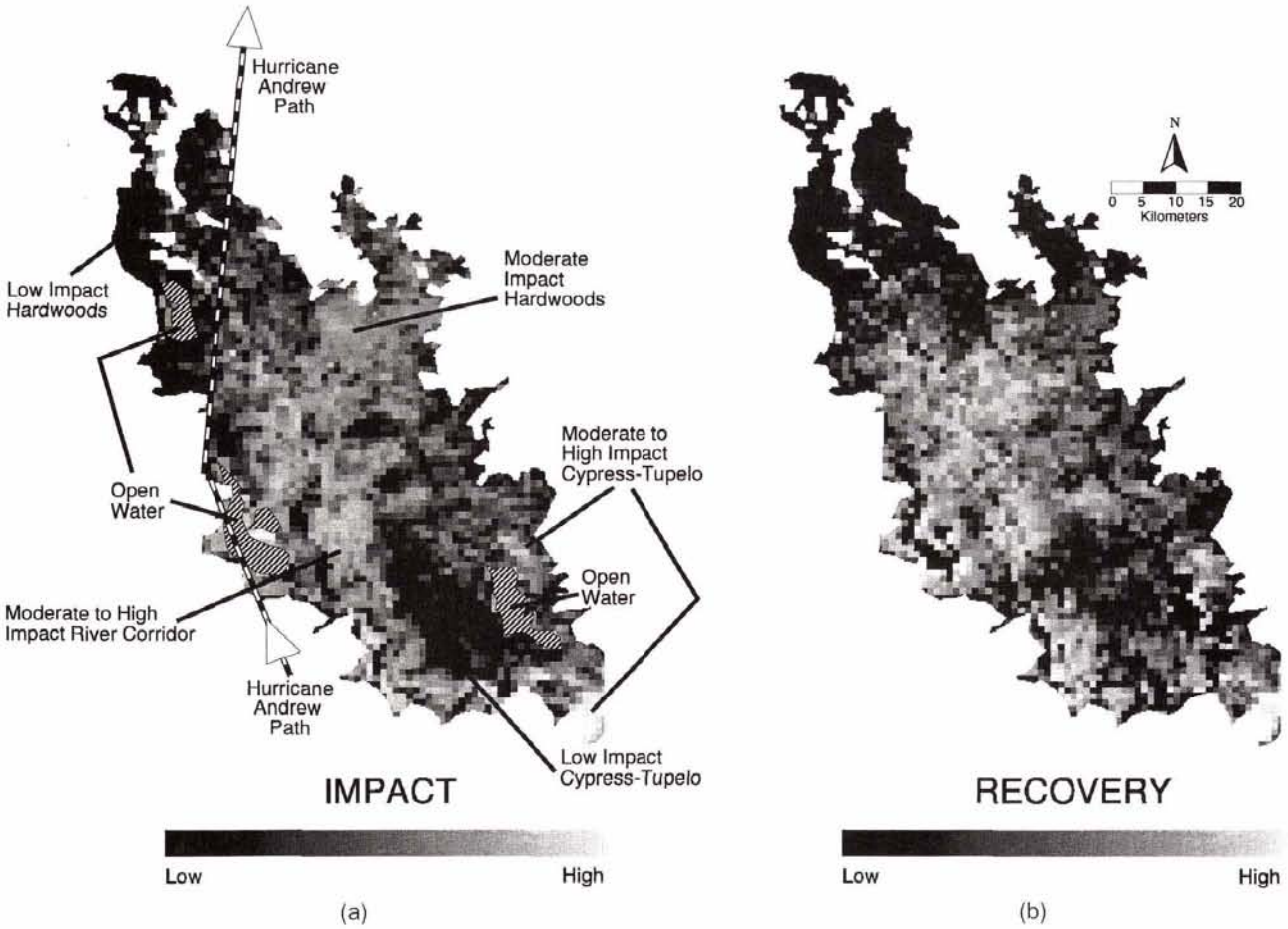

Figure 1. (a) The distribution of hurricane impact to the forested areas. Impact magnitude was estimated by differencing the June and August (3 days after the hurricane passage) NDVI images. The central track of the hurricane and regions specifically addressed in the text are depicted. (b) Recovery magnitude was estimated by differencing the October and the August NDVI images.

Even though separated by forest type, these statistical measures describe basin-wide relationships; a spatial component is not an explicit part of the statistical description. The overlay procedure allowed the spatial component to be incorporated along with forest type into the analysis. Finally, to help clarify the associations, impact and recovery magnitudes were grouped into class intervals.

Proportions of forest type per impact magnitude remained nearly constant within the impact interval of 0 to 20, representing little to no impact (Table 1). In this interval, hardwood percentages were slightly higher ($p = 0.0034$) than cypress-tupelo percentages. At values representing higher impacts (>10), the relative proportions of forest type changed. From 20 to 30, cypress-tupelo percentages were significantly higher ($p = 0.0132$) than from 10 to 20, while hardwood percentages were significantly lower ($p = 0.1038$). The percentages of cypress-tupelo and hardwood remained nearly constant above 25 and up to 30. Open forest percentages increased within the 20 to 25 interval relative to lower or higher impact ranges.

Forest type proportions related to recovery magnitudes followed a somewhat opposite trend than did the distribution related to impact magnitudes. Hardwood and cypress-tupelo percentages were about equal and were constant in the recovery intervals spanning 0 to 15. From 15 to 20, however, there was an increase in the hardwood percentages and, conversely, a decrease in cypress-tupelo percentages. The open canopy percentages decreased from 10 to 15, and then remained nearly constant.

Within the overall trend of forest-type percentage with impact and recovery magnitude, 50 pixels defining an area dominated by cypress-tupelo in the southeast corner of the basin stood out. Twenty-nine of these 50 pixels were related to impact values above 30. Thirty of these 50 pixels were related to recovery values above 25. The only significant change in the analyses of proportions when excluding these values was associated with the range of impacts above 30.

Discussion

Statistical measures describing the distributions of forest type (hardwood, cypress-tupelo, and open canopy mix) with impact and recovery magnitudes suggested fairly equal impact averages for all forest types but a lower recovery magnitude for hardwood than cypress-tupelo and open forests. The univariate statistics are generalized for the entire basin (impact and nonimpact pixels) and could not be used directly to relate the spatial distribution of impact and recovery magnitudes to the distribution of forest type. Visual interpretation and comparison of the classified map to the impact and recovery maps helped clarify the forest response to the hurricane impact, such as in the case of the spatial covariation between high impacts and recovery magnitudes and corri-

TABLE 1. IMPACT AND RECOVERY OF FOREST TYPE.

		Forest Type							
		Hardwood				Cypress-Tupelo		Open Canopy	
		Impact		Recovery		Impact	Recovery	Impact	Recovery
ΔNDVI	Scaled ΔNDVI	*n*	Mean ± SE	*n*	Mean ± SE	Mean ± SE	Mean ± SE	Mean ± SE	Mean ± SE
≤−0.08	≤10	9	25.18 ± 9.13	246	49.44 ± 1.93	52.10 ± 6.44	38.11 ± 1.35	22.72 ± 5.07	12.45 ± 0.95
−0.08 to −0.04	−10 to −5	36	55.92 ± 5.71	134	49.96 ± 2.59	27.63 ± 3.34	36.95 ± 1.61	16.44 ± 4.10	13.09 ± 1.34
−0.04 to 0.00	−5 to 0	133	51.08 ± 3.21	182	36.94 ± 2.35	33.25 ± 2.03	45.10 ± 1.64	15.67 ± 1.81	17.96 ± 1.30
0.00 to 0.04	0 to 5	508	46.70 ± 1.58	336	42.63 ± 1.85	38.92 ± 1.07	41.83 ± 1.28	14.38 ± 0.75	15.55 ± 0.90
0.04 to 0.08	5 to 10	1107	45.75 ± 1.00	399	36.35 ± 1.56	40.98 ± 0.70	47.01 ± 1.16	13.26 ± 0.46	16.64 ± 0.81
0.08 to 0.12	10 to 15	959	47.40 ± 0.95	462	45.27 ± 1.49	40.53 ± 0.69	41.28 ± 1.07	12.08 ± 0.40	13.46 ± 0.65
0.12 to 0.16	15 to 20	426	47.92 ± 1.40	475	52.41 ± 1.36	39.32 ± 0.98	37.38 ± 0.98	12.77 ± 0.65	10.21 ± 0.56
0.16 to 0.20	20 to 25	102	35.66 ± 2.52	484	52.33 ± 1.36	49.39 ± 2.02	36.81 ± 0.97	14.95 ± 1.24	10.86 ± 0.60
0.20 to 0.24	25 to 30	19	39.12 ± 5.63	335	48.45 ± 1.67	51.67 ± 4.85	39.55 ± 1.19	9.21 ± 2.32	12.00 ± 0.76
>0.24	>30	60	19.71 ± 2.33	206	40.83 ± 2.07	63.16 ± 2.37	44.60 ± 1.54	17.13 ± 2.82	14.58 ± 1.15

Note: *n* = Number of observations in each class interval. All three forest types have the same number of observations per impact and recovery class.
Mean = Mean of the proportion of forest type in each pixel within the described class interval.
SE = Standard error.
Negative NDVI reveal that August values are larger than those of June.

dors along the waterways dominated by willows and mixed forests.

In general, visual comparison supported the post-hurricane reconnaissance of the area (Kelly, 1993; Doyle *et al.*, 1995). These surveys suggested that most forest damage occurred in the primarily hardwood-dominated northern areas of the basin, while less effect was noted in the southeastern basin that is dominated by cypress-tupelo. Clearly identified in this study were areas of moderate to high impact in the hardwood-dominated area in the northern basin and low to moderate impacts in the cypress-tupelo-dominated area in the southcentral region of the basin. This dominantly cypress-tupelo area suffered some of the lowest impacts even though near and to the right of the hurricane track.

In addition, however, visual comparison identified a dominantly cypress-tupelo area in the southeast corner of the basin that suffered some of the highest impacts and was related to some of the highest recoveries. Conversely, a mostly hardwood area to the northwest of the basin was identified that sustained some of the lowest impacts even though near the center of the storm track. Both the areas of high cypress-tupelo impacts and low hardwood impacts were identified within the forested area but outside the legal boundaries of the Atchafalaya River basin, and, most likely, were not included in the early reconnaissance of the area (Kelly, 1993; Doyle *et al.*, 1995). It is possible, because of the spatial variation of hurricane intensity and stand characteristics (Doyle *et al.*, 1995), that the area of low hardwood impacts experienced relatively lower wind speeds and the area of high cypress-tupelo impacts experienced relatively higher wind speeds.

Overlay of the 1-km impact and recovery maps onto the 25-m classified map allowed examination of the spatial covariation of the changes in forest-type percentages and impact and recovery magnitudes. Analyses of the data resulting from the overlay procedure suggest that forests with a somewhat higher percentage of hardwood than cypress-tupelo and around 13 percent open forest dominated the low impact range. This range of impacts also contained the largest fraction of impacted forest. At moderate to high impacts, cypress-tupelo forest percentages within the 1-km integrated areas were substantially higher than were the hardwood percentages; the highest impacts occurred in an area dominated by cypress-tupelo. The open forest percentage also had a substantial increase at moderate impact magnitudes, probably reflecting the destruction to willows and mixed forest along the river corridors. Investigation of forest-type proportions integrated over the 1-km recovery pixels indicated that forest with nearly equal hardwood and cypress-tupelo percentages were associated with low to moderate recovery magnitudes. Higher recoveries were more likely to be related to forest with a somewhat higher percentage of hardwoods than cypress-tupelo and about 10 percent to 14 percent open forest.

These results suggest that some cypress-tupelo forests were highly impacted and that, on average, these forests were more likely to be associated with high impact magnitudes than were hardwood forests. If cypress-tupelos are more resistant to wind damage than are hardwoods, as suggested by earlier studies, the relation to higher impacts could be an artifact of the non-singular relationship between impact magnitude and damage type or a consequence of the windfield distribution. Higher impacts probably represent a mixture of severe and somewhat lessor damage. If severe damage was dominantly associated with hardwoods, then, as the percentages of hardwoods decreased at higher impact magnitudes as shown in this study, the severity of impact to the hardwoods would have to increase. In fact, in at least one region of the basin, this was not the case. Some of the highest impacts were identified in an area of almost solely cypress-tupelo; thus, higher impact magnitudes were not solely a function of hardwood damage severity. Again, if cypress-tupelo were more resistant to wind damage than were hardwood, higher impacts could be a result of higher or longer duration wind speeds. Without a windfield distribution, however, this aspect of the impact spatial distribution could not be examined.

Even though the spatial distribution of recovery generally supported the impact spatial distribution, the spatial variation in recovery and impact magnitudes did not necessarily covary. High impacts could be associated with high or low recoveries. Higher percentages of hardwood within the 1-km spatial integration were more likely to be associated with a higher recovery magnitude than forests with a higher percentage of cypress-tupelo. This could support the overall trend of lower impacts related to higher percentages of hardwoods; however, in areas of dramatic losses in overstory canopy, lower canopy cover could have flourished for a few months, affecting the recovery magnitude.

Conclusion

Using an NDVI transform, a suite of high temporal frequency AVHRR data was used to estimate impact and recovery magni-

tudes at a 1-km spatial scale for a wetland forest affected by a hurricane. Impact and recovery distributions were statistically, visually, and with an overlay procedure compared to a landcover map derived from 25-m TM data. In general, the recovery spatial distribution followed the impact spatial distribution; however, even though spatially coincident, the recovery and impact magnitudes did not necessarily covary. Spatial covariation analysis suggested hardwood percentages increased from the low to moderate and high recovery ranges and, conversely, cypress-tupelo percentages decreased.

Comparison of the impact spatial distribution with the classified land-cover map found the same regions of moderate to high impacts in the hardwoods of the northern basin and low impacts in the cypress-tupelos of the southcentral basin as reported by earlier studies. These results supported earlier suggestions that hardwoods were more susceptible to wind damage than were cypress-tupelos. Conversely, this study also identified previously unreported regions of low impacts dominated by hardwoods and high impacts dominated by cypress-tupelo. These associations do not fit the suggested relationship between severity of impact and hardwoods. In addition, the spatial covariation of impact and forest type analysis showed that, while hardwood and cypress-tupelo percentages remained nearly equal and constant at lower impact values, there was a distinct increase in cypress-tupelo and decrease in hardwood percentages at moderate to high impacts. Further, by revealing the overall spatial distribution of impact magnitudes, this study documented the spatial covariation between higher impacts and river corridors dominated by willows and mixed forests, as well as the widespread distribution of low to moderate impacts throughout the central region of the basin. Results of this study do not necessarily dispute earlier suggestions that hardwoods are more susceptible to wind damage than are cypress-tupelo. Superimposing the windfield on the site and stand characteristics may assist in determining the reason for the severity of impact. Future analyses will examine the spatial covariance of wind speeds and duration and forest type and impact.

The appeal of the technique used in this study is that it used common image processing systems and a simple method to transfer the knowledge gained at one scale (e.g., AVHRR) to another scale (e.g., TM) in a way useful to resource managers. This uncomplicated approach produced a spatial and temporal detection system that created an added level of information not available from either sensor system individually.

Acknowledgments

The authors thank Dr. John Kelly and Dr. David Evans of the U.S. Forest Service, Southern Forest Experiment Station for access to videography of post-Hurricane Andrew damage and the forest inventory and analysis information within the Atchafalaya Basin. The authors thank Dr. Emery for providing the AVHRR NAVIGATE software and support in its use. We thank Ms. Beth Vairin and Mr. Daryl McGrath of the National Wetlands Research Center for editing this manuscript. Finally, we thank the anonymous reviewers for their time and effort.

References

Andres, L., W. Salas, and D. Skole, 1994. Fourier analysis of multitemporal AVHRR data applied to a land cover classification, *International Journal of Remote Sensing*, 15:1115–1121.

Chavez, P., and D. MacKinnon, 1994. Automatic detection of vegetation changes in the southwestern United States using remotely sensed images, *Photogrammetric Engineering & Remote Sensing*, 60:571–583.

Congalton, R., 1988. A comparison of sampling schemes used in generating error matrices for assessing the accuracy of maps generated from remotely sensed data, *Photogrammetric Engineering & Remote Sensing*, 54:593–600.

———, 1991. A review of assessing the accuracy of classifications of remotely sensed data, *Remote Sensing of Environment*, 37:35–47.

Doyle, T., B. Keeland, L. Gorham, and D. Johnson, 1995. Structural impact of Hurricane Andrew on the forested wetlands of the Atchafalaya Basin in south Louisiana, *Journal of Coastal Research*, 21:354–364.

Eastman, J., and M. Fulk, 1993. Long sequence time series evaluation using standardized principal components, *Photogrammetric Engineering & Remote Sensing*, 59:1307–1312.

Ehrlich, D., J. Estes, and A. Singh, 1994. Applications of NOAA-AVHRR 1 km data for environmental monitoring, *International Journal of Remote Sensing*, 15:145–161.

Eidenshink, J., 1992. The 1990 conterminous U. S. AVHRR data set, *Photogrammetric Engineering & Remote Sensing*, 58:809–813.

Janssen, L., and F. van der Wel, 1994. Accuracy assessment of satellite derived land-cover data: A review, *Photogrammetric Engineering & Remote Sensing*, 60:419–426.

Jensen, J., E. Ramsey III, H. Mackey, E. Christensen, and R. Sharitz, 1987. Inland wetland change detection using aircraft MSS data, *Photogrammetric Engineering & Remote Sensing*, 53:521528.

Jensen, J., D. Cowen, J. Althausen, S. Narumalani, and O. Weatherbee, 1994. An evaluation of the coastwatch change detection protocol in South Carolina, *Photogrammetric Engineering & Remote Sensing*, 59:1039–1046.

Kelly, J., 1993. Hurricane Andrew forest damage assessment, *World Resource Review*, 5:401–408.

Lulla, K., and P. Mausel, 1983. Ecological applications of remotely sensed multispectral data, *Remote Sensing of the Environment* (B. F. Richasen, Jr., editor), Hunt, Dubuque, Iowa, pp. 354–377.

Moody, A., and C. Woodcock, 1994. Scale-dependent errors in the estimation of land-cover proportions: Implications for global land-cover datasets, *Photogrammetric Engineering & Remote Sensing*, 60:585–594.

PCI Inc., 1993. *Using PCI Software, Version 5.2 EASI/PACE*, PCI Inc., Richmond Hill, Ontario, Canada.

Ramsey III, E., D. Chappell, and D. Baldwin, 1997. AVHRR imagery used to identify Hurricane Andrew damage in a forested wetland of Louisiana, *Photogrammetric Engineering & Remote Sensing*, 63:293–297.

Ramsey III, E., and S. Laine, 1997. Comparison of Landsat Thematic Mapper and high resolution photography to identify change in complex coastal wetlands, *Journal of Coastal Research*, 13:281–292.

Ripple, W., 1994. Determining coniferous forest cover and forest fragmentation with NOAA-9 Advanced Very High Resolution Radiometer Data, *Photogrammetric Engineering & Remote Sensing*, 60:533–540.

Rosborough, G., D. Baldwin, and W. Emery, 1994. Precise AVHRR navigation, *IEEE Transactions on Geoscience and Remote Sensing*, 32:644–657.

Roughgarden, J., S. Running, and P. Matson, 1991. What does remote sensing do for ecology? *Ecology*, 72:1918–1922.

Samson, S., 1993. Two indices to characterize temporal patterns in the spectral response of vegetation, *Photogrammetric Engineering & Remote Sensing*, 59:511–517.

Settle, J., and N. Drake, 1993. Linear mixing and the estimation of ground cover proportions, *International Journal of Remote Sensing*, 14:1159–1177.

Wickland, D., 1991. Mission to planet Earth: the ecological perspective, *Ecology*, 72:1923–1933.

Zhu, Z., and D. Evans, 1994. U. S. forest types and predicted percent forest cover from AVHRR data, *Photogrammetric Engineering & Remote Sensing*, 60:525–531.

Received 7 June 1997; revised and accepted 25 September 1997; revised 8 December 1997)